Direct Observation of Self-Focusing with Subdiffraction Limited Resolution Using Near-Field Scanning Optical Microscope

Ki-Bong Song,* Jaekwang Lee, Jong-Hoi Kim, and Kyuman Cho
Department of Physics, Sogang University, 1 Sinsoo-Dong, Mapo-Ku, Seoul, 121-742, Korea

Soon-Kwang Kim
Materials Design Laboratory, Korea Institute of Science and Technology, P.O. Box 131, Cheongryang, Seoul 130-650, Korea
(Received 13 December 1999)

The self-focusing effect in As_2S_3 glass has been studied using a near-field scanning optical microscope. Optical images of fine features in the self-focused beam were directly measured at the self-focus with approximately 100 nm spatial resolution. Because of the unusually large nonlinear refractive index at 690 nm, filaments with minimum size of 0.3 μm were observed in a 1.6 mW beam propagating through the 1.7 μm thin film. A qualitative analysis of our experimental results is presented. We show that nonparaxiality is responsible for arresting self-focusing, as predicted by recent theories.

PACS numbers: 61.16.Ch, 07.79.Fc, 42.65.Jx

Self-focusing (SF) due to the nonlinear optical Kerr effect has been studied extensively by many authors [1–5]. One of the main purposes of previous work was to find out how SF is arrested and how small the diameter of the self-focused beam could be. Although many important features of SF mechanisms have been revealed, as Semenov *et al.* point out, the final stage of SF is still an open question [2]. Recent theoretical work shows that nonparaxiality arrests SF and results in a beam size on the order of the wavelength beam size, even though linear and nonlinear saturation mechanisms are absent [3,4]. On the other hand, Semenov *et al.* have shown that a needle of light with a channel width much smaller than the wavelength can be obtained with extreme concentration of radiation power [2].

Until now, experimental schemes for observing SF effects relied on far-field imaging techniques [1,5], in which the fine structure of the self-focus may not be observed. Near-field scanning optical microscopy (NSOM), which has been applied for studying various linear and nonlinear optical effects with subdiffraction limited resolution [6], is an ideal technique for high resolution study of SF effects. However, it is very difficult to use NSOM in SF measurements because, in general, a high power laser beam is necessary to overcome the diffraction effects in the propagating narrow optical beam, and a self-focused high power laser beam can damage the tip and/or cause thermal instability in the distance regulation process. Therefore, in order to study SF effects with NSOM, it is essential to use a material that has a very high third order nonlinear index and small linear and nonlinear losses.

An arsenic trisulfide (As_2S_3) glass is an ideal material for studying SF with NSOM, because it has very large third order nonlinear susceptibility when the pump beam wavelength is contained in the Urbach tail region [7,8], where the linear absorption coefficient decreases exponentially with the energy difference between the band gap energy E_g and the photon energy $h\nu$ of the pump beam. The linear absorption of As_2S_3 glass in this region is very small ($\sim$1–10 cm^{-1}) and easily saturated by low power illumination [9]. It has been shown that the nonlinear refractive index n_2 of the As_2S_3 glass induced by 633 nm He-Ne laser, whose photon energy falls into the Urbach tail region, has an 8 orders of magnitude larger value than n_2 measured using near infrared light as a pump source [7,8,10,11]. For example, using a Z-scan scheme, a well known technique for measuring the third order nonlinear refractive index [12], an extremely large n_2, 8.65×10^{-10} m^2/W, was observed with a 633 nm He-Ne laser [7], while smaller, but still approximately 2 orders of magnitude larger n_2 than that of silica glass 2.5×10^{-18} m^2/W, was obtained in a Z-scan measurement using a Q-switched, 1.06 μm Nd:YAG laser [10].

The n_2 of the as-evaporated unannealed 1.7 μm thick As_2S_3 film was measured at 690 nm pump wavelength using the Z-scan arrangement and theory given in Ref. [12]. The measured value of n_2 is $\sim 2.64 \times 10^{-10}$ m^2/W, which is in good agreement with the results reported in Refs. [7] and [8]. On the other hand, we found that the nonlinear susceptibility value observed in our Z-scan measurements is additively increased in each consecutive measurement as shown in Fig. 1. The increase in nonlinear susceptibility reaches saturation after 70 measurement cycles. The nonlinear index given above was measured after this saturation. We believe that the cumulative effects and saturation characteristics in the Z-scan measurements are due to the photoinduced effects (PIE) caused by subband gap ($h\nu < E_g$) illumination, such as the photodarkening effect (PDE), photoexpansion effect, and so forth [9,13]. The PDE, reduction of band gap caused by subband gap or band gap ($h\nu > E_g$) illumination, leads to a concomitant change in refractive index [9,14]. Therefore, a permanent graded index (GRIN) can be written in the film in the Z-scan procedure. It can be argued which value of n_2 should be used for nonlinear index: n_2 measured in the first scan or n_2 measured after saturation.

 0031-9007/00/85(18)/3842(4)$15.00

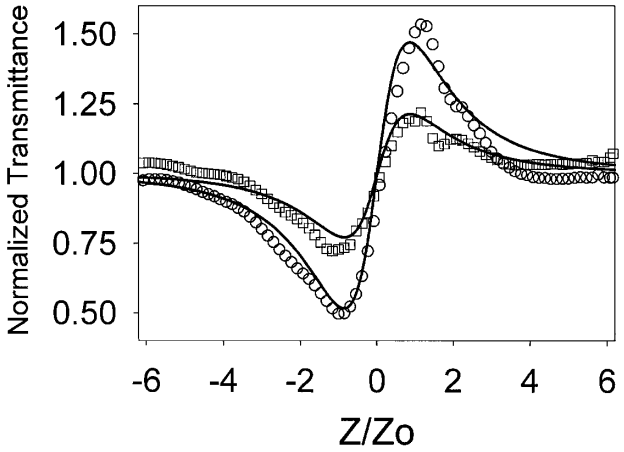

FIG. 1. Closed aperture Z-scan curves. In the figure, squares and circles represent experimental results after 40 measurement cycles and 70 measurement cycles, respectively. Solid lines are the corresponding best fits to the theory.

We believe that the correct value of n_2 can be measured after saturation if the GRIN effect is taken into account. However, the order of magnitude of the value of n_2 measured after saturation is still valid without GRIN effect correction, because our experimental result on self-focusing is in good agreement with a numerical model given by Feit and Fleck [3] for $n_2 \sim 10^{-10}$ m^2/W.

Regarding the linear and nonlinear optical characteristics mentioned above, we can see that As_2S_3 in an ideal material for studying SF with NSOM. The critical power for SF is approximately 270 μW for $n_2 = 10^{-10}$ m^2/W, which implies that SF can be easily observed in very short interaction lengths with a low power continuous wave laser. In addition, linear and nonlinear loss in the film can be ignored because of the short interaction length, small absorption coefficient, and low cw optical power. In our current work, we were able to observe filament formation in the 1.7 μm As_2S_3 thin film at 1.6 mW optical power.

A schematic of our experimental arrangement for SF measurement is shown in Fig. 2. In most of our measurements, we used an InGaAlP semiconductor laser as a source, because the lasing wavelength, 690 nm, is ideal for studying SF: it has very small linear absorption but very large n_2. Although the lasing wavelength is close to the band gap of As_2S_3, 605 nm, and have large linear absorption, we also used a 2 mW, 633 nm He-Ne laser to study SF with an axially symmetric Gaussian beam. In either case, the laser beam was properly expanded and focused into the film through a slide glass substrate using a 0.1 numerical aperture microscope objective lens. Making use of the Z-scan technique, we were able to locate the focus inside the thin film. The transmitted beam at the surface of the film was profiled using transmission geometry NSOM. We used metal coated fiber tips with approximately 100 nm aperture. The distance between the tip and the surface was maintained at $\sim$10 nm using the tuning fork scheme for shear-force measurement [15]. The laser beam was intensity modulated and the beam transmitted through the film was picked up by the fiber tip and sent to a photodiode. The detected signal was processed by a lock-in amplifier synchronized to the laser modulation frequency.

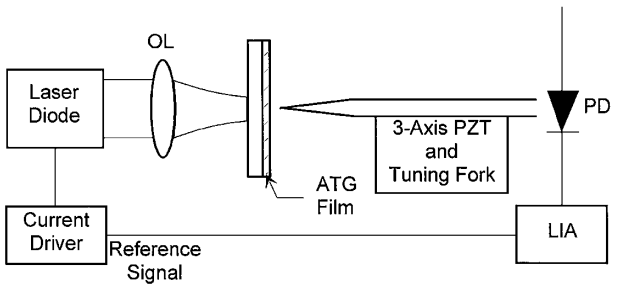

FIG. 2. Experimental arrangement. In the figure, LIA, OL, and PD represent lock-in amplifier, microscope objective lens, and photodiode, respectively.

The optical image of the laser beam focused onto the region of the glass side surface, which was not coated with the As_2S_3 film, is shown in Fig. 3(a). This figure shows the optical image of the focused output beam from the asymmetric rectangular wave guide structure of the active area of the semiconductor laser. Figure 3(b) is the near-field optical image of the 1.6 mW focused beam after passing through the As_2S_3 film. In this image, we can see significant beam size reduction. Moreover, three bright maxima appear in the region specified with the dotted box

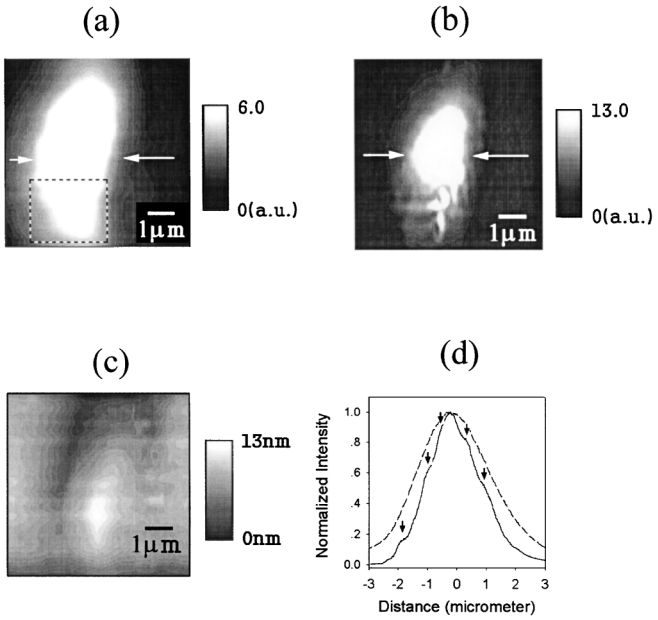

FIG. 3. Optical images at 1.6 mW: (a) the image was taken at the glass side where the film was not coated, (b) image of the output beam at the As_2S_3 film surface. Geometrical lens structure caused by the photoexpansion effect at 4.8 mW is shown in (c), and the line scan images taken along the directions specified by the corresponding arrows in (a) and (b) are shown in (d).

in the figure. These bright spots were not caused by the light scattering from local defects or dust particles, because we cannot see any correlated topographical structure in the shear-force image. In fact, although a minor convex lens structure caused by the photoexpansion effect was barely observable, we could not find any significantly noticeable feature in the topography in the case of 1.6 mW illuminating light power. Lens structure formed by the photoexpansion effect [13] was noticeable only at 4.8 mW illumination power as shown in Fig. 3(c). The geometrical lens structure, however, could not produce any influence on the NSOM image, because not only was the height of the topography negligibly small ($\sim$13 nm), but also the optical image was taken when the tip was scanning over the surface with approximately 10 nm constant gap distance. The region where the bright spots are present in Fig. 3(b) corresponds approximately to the region specified in the dotted box in Fig. 3(a). It can be seen in the figure that the beam in this region is narrower than the other region, or, in other words, it has bigger local intensity variations than the other region. Therefore, we believe that bright spots in Fig. 3(b) are filaments developed in this region. Beam width along the short axis of a filament is less than 0.3 μm, which cannot be identified using a conventional far-field imaging technique. To the best of our knowledge, this is the first image that shows an actual self-focused area with subdiffraction limited resolution.

In the case of the optical beam located outside the dotted box Fig. 3(a), i.e., an optical beam that did not contribute to filament formation, we can see a significant beam size reduction in comparison with the input optical beam image [Fig. 3(a)]. At least 30% reduction of beam size can be found in the line scan images shown in Fig. 3(d). The line scan images were taken along the corresponding lines specified in Figs. 3(a) and 3(b), respectively. Using the representation for a Gaussian beam propagating through a GRIN medium [16] and the parameters given in Ref. [14], we found that the GRIN profile results in at most 18% beam size reduction. Therefore, we can see that both GRIN and the nonlinear optical SF effect play major roles in beam size reduction. The line scan image of the output beam from the As_2S_3 film [the solid line in Fig. 3(d)] shows distortions at the locations marked as downward arrows. Although we have not been able to explain the reasons for the distortions, we believe these distortions did not originate from the interference caused by multiple reflections in the film, because otherwise they would occur as local maxima and minima. We will show that side lobes will develop for higher power illumination at the locations where the distortions occur.

An optical image taken at 4.8 mW illumination power is shown in Fig. 4(a). The beam is focused into one bright spot with several side lobes. The corresponding shear-force image in Fig. 3(c) does not show any topographical structures correlated with the bright spot in the optical image. We believe that the bright spot in Fig. 4(a) is formed by the SF effect of the portion of the input beam

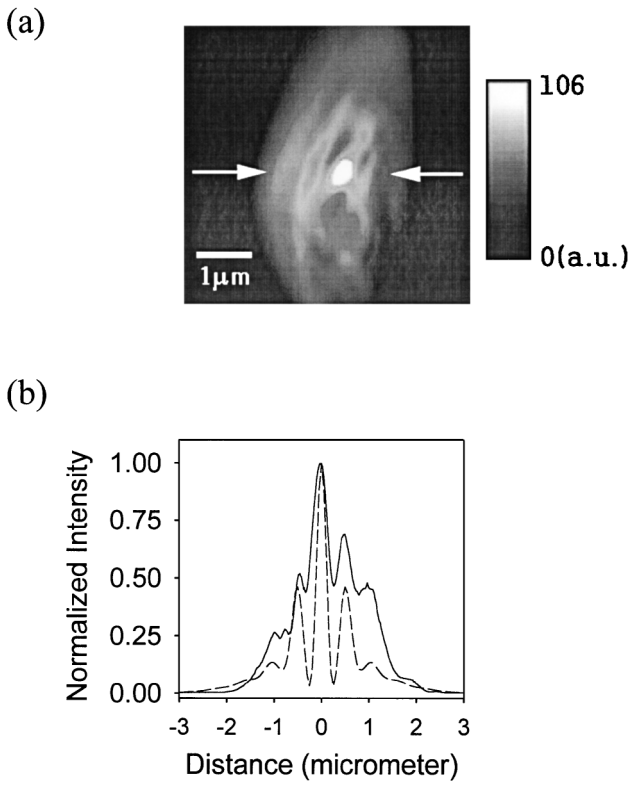

FIG. 4. Optical image at 4.8 mW input power (a), and the line scan images (b). Solid line and dotted line in (b) represent line scan images taken along the direction specified by the pair of arrows shown in (a) and the numerical calculation, respectively.

located approximately in the region outside the dotted box in Fig. 3(a). In case of 7.2 mW input power, we found that the defocused and focused areas in Fig. 4(a) were refocused into one spot and defocused as predicted by Feit and Fleck [3]: The self-focused beam undergoes a defocusing and focusing cycle while the beam propagates through the nonlinear medium.

The line scan image, the solid line in Fig. 4(b), shows that side lobes around the self-focused beam are formed in the corresponding regions marked with arrows in Fig. 3(d), which is further evidence that the bright spot and side lobes in the figure are developed by the SF effect. The line scan was made along the direction given by the pair of arrows shown in Fig. 4(a). Recent theoretical work has shown that the self-focused beam evolves into concentric rings or ripples when it defocuses, and they refocus into a solid spot in the next self-focusing cycle: the beam undergoes focusing and defocusing cycles until it finally defocuses [3,4]. We believe that, because of the asymmetry of the propagating beam, the self-focused beam is broken into the side lobes but not into concentric rings.

Although the GRIN structure induced by PDE can accelerate the SF process in the initial stage, since the size of the self-focus is much smaller than the characteristic size of the GRIN, it cannot contribute any significant effect at the self-focus. We found that our experimental result at 4.8 mW input power can be explained qualitatively by the

use of the numerical model given by Feit and Fleck. The dotted line curve in Fig. 4(b) is the theoretical line scan plot using the numerical model, which is in good agreement with our experimental result (the solid line). In the calculation, we used actual experimental parameters, except a perfect Gaussian input beam was assumed. The theoretical line scan result was obtained from the concentric image of the numerical plot.

The shear-force image shown in Fig. 3(c) represents the topographical structure of the surface where the optical image, Fig. 4(a), was taken. Elliptic, convex structure in the middle part of the shear-force image is the optically induced lens structure caused by the photoexpansion effect. It is interesting to notice that the topographical image in Fig. 3(c) follows the output beam shape approximately, which could be given as the optical image in the absence of filaments. It has been shown that the PIE due to subband gap illumination results in structural change which has approximately the same profile as the illuminating light. We think that the shear-force image did not show detailed structure of the filaments because of the finite resolution of the PIE, which may be given by the finite diffusion length of optically generated electron-hole pairs before they form a self-trapped exciton.

In case of SF with a 2 mW He-Ne laser, although the near-field images are not shown here, no other special features were observed. The beam size, however, reduced by almost 40%. We found that the SF image fits very well to the numerical model. We found, however, the alignment was critical to obtain circularly symmetric SF: any noncentro symmetric intensity distribution caused by slight misalignment distorts the image because of the extremely high n_2 of As_2S_3 at 633 nm. We also could not observe any significant interferences caused by multiple reflections in the film interface.

In summary, the SF effect in As_2S_3 thin films has been studied using NSOM. High spatial resolution images of self-focused areas have been obtained and analyzed at various input optical powers. We have shown that GRIN structure written by PDE can contribute to the beam size reduction in the initial stage of SF. The GRIN contribution, however, gets smaller while the beam is focusing, and exhibits negligible effects at the self-focus. The minimum beam size obtained at 4.8 mW input beam power, which is approximately 18 times bigger than the critical power for the SF effect, was less than 0.3 μm, which is approximately equal to the wavelength of light in the film (0.265 μm). Our experimental results are in good agreement with recent theoretical work, which indicates that nonparaxiality arrests SF at the power levels used in our experiment.

The authors thank Professor C. C. Davis and Dr. I. Smolynianov of the University of Maryland for helpful comments in analyzing experimental results. We also thank Professor Sung-Ho Shin of Kangwon University for helping us with preparing as-evaporated As_2S_3 thin films. Part of this research has been supported by the Ministry of Science and Technology under the National Research Laboratory Program.

*Present address: Material Design Laboratory, Korea Institute of Science and Technology, P.O. Box 131, Cheongryang, Seoul 130-650, Korea.

[1] Y. R. Shen, *The Principles of Nonlinear Optics* (Wiley, New York, 1984), and references therein.
[2] V. E. Semenov, N. N. Rozanov, and N. Y. Vysotina, J. Exp. Theor. Phys. **89**, 243 (1999).
[3] M. D. Feit and J. A. Fleck, Jr., J. Opt. Soc. Am. B **5**, 633 (1988).
[4] G. Fibich, Phys. Rev. Lett. **76**, 4356 (1996).
[5] I. A. Al-Saidi, J. Phys. D **32**, 874 (1999); M. L. Dowell, R. C. Hart, A. Gallagher, and J. Cooper, Phys. Rev. A **53**, 1775 (1996); K. D. Dorkenoo, A. J. van Wonderen, and G. Rivoire, J. Opt. Soc. Am. B **15**, 1762 (1998).
[6] K. B. Song, J. E. Bae, K. Cho, S. Y. Yim, and S. H. Park, Appl. Phys. Lett. **73**, 2260 (1998); I. I. Smolyaninov, D. L. Mazzoni, and C. C. Davis, Phys. Rev. Lett. **77**, 3877 (1996); I. I. Smolyaniov, C. H. Lee, C. C. Davis, and S. Rudin, J. Microsc. **194**, 532 (1999), and references therein.
[7] Y. J. Sohn, Y. L. Lee, C. H. Kwak, and O. S. Choe, SPIE Opt. Sci. New Technol. **2778**, 800 (1996); S. G. Kim, Y. L. Lee, C. H. Kwak, O. S. Choe, Y. W. Lee, J. B. Song, H. H. Suh, and B. Lee, J. Opt. Soc. Korea (Korean ed.) **9**, 342 (1998).
[8] C. H. Kwak, J. T. Kim, and S. S. Lee, Opt. Lett. **13**, 437 (1988); T. Yanagisawa, S. Ohsawa, and H. Kuribayasgi, U.S. Patent No. 5615206 (1997).
[9] H. Fritzsche, Philos. Mag. B **68**, 561 (1993); H. Fritzsche, Solid State Commun. **99**, 153 (1996); V. K. Tikhomirov, P. Lievens, N. Qamhieh, and G. J. Adriaenssens, J. Non-Cryst. Solids **198–200**, 119 (1996).
[10] F. Smektala, C. Quemard, L. Leneindre, J. Lucas, A. Barthelemy, and C. De Angelis, J. Non-Cryst. Solids **239**, 139 (1998).
[11] D. W. Hall, M. A. Newhouse, N. F. Borrelli, W. H. Dumbaugh, and D. L. Weidman, Appl. Phys. Lett. **54**, 3 (1989); M. Asobe, K. Suzuki, T. Kanamori, and K. Kubodera, Appl. Phys. Lett. **60**, 1153 (1992); E. Hajto, P. J. S. Ewen, and A. E. Owen, Non-Cryst. Solids **164–166**, 901 (1993); H. Kobayashi, H. Kanbara, and M. Koga, J. Appl. Phys. **74**, 3683 (1993); H. Kanbara, S. Fujiwara, and K. Tanaka, Appl. Phys. Lett. **70**, 925 (1997).
[12] M. Sheik-Bahae, A. A. Said, T. H. Wei, D. J. Hagan, and E. W. Van Stryland, IEEE J. Quantum Electron. **26**, 760 (1990); B. K. Rhee, J. S. Byun, and E. W. Van Stryland, J. Opt. Soc. Am. B **13**, 2720 (1996).
[13] H. Hisakuni and K. Tanaka, Opt. Lett. **20**, 958 (1995); Science **270**, 974 (1995).
[14] H. Hisakuni and K. Tanaka, Solid State Commun. **90**, 483 (1994); S. Ramachandran, S. G. Bishop, J. P. Guo, and D. J. Brady, IEEE Photonics Technol. Lett. **8**, 1041 (1996).
[15] A. G. T. Ruiter, J. A. Veerman, K. O. van der Werf, and N. F. van Hulst, Appl. Phys. Lett. **71**, 28 (1997).
[16] R. Falciai and T. Pascucci, Appl. Opt. **31**, 5211 (1992).